SIMULTANEOUS VELOCITY AND REFLECTIVITY INVERSION: FWI + LSRTM

Y. Yang[1], J. Ramos-Martinez[1], D. Whitmore[1], G. Huang[1], N. Chemingui[1]

[1] PGS

Summary

We present an iterative non-linear inversion method to simultaneously estimate both velocity and reflectivity. The core of the inversion workflow is a full acoustic wavefield modeling relation parameterized in terms of velocity and vector reflectivity. A key aspect is the separation of the low- and high-wavenumber components of the gradient based on inverse scattering theory, enabling the sensitivity kernels to update the velocity and the vector reflectivity, respectively. The estimation problem is formulated as a multi-parameter adjoint-state inversion where the trade-off between velocity and reflectivity is minimized through scale separation. Our approach is equivalent to performing Full Waveform Inversion (FWI) and Least-Squares Reverse Time Migration (LSRTM) in a single framework using the full wavefield. The output of the inversion is a detailed velocity model together with an accurate estimate of the earth reflectivity with compensation for incomplete acquisition, poor illumination, and multiple crosstalk. The new approach reduces the turnaround time of imaging projects by combining velocity model building (FWI) and imaging (LSRTM) into a single inversion process with minimal data pre-processing.

Simultaneous velocity and reflectivity inversion: FWI + LSRTM

Introduction

The main goal of seismic prospecting is detailed estimation of subsurface properties, primarily velocity and reflectivity. The classic imaging workflow includes two sequential tasks based on scale separation; building a velocity model (long wavelength model), and imaging the subsurface reflectivity associated with geological boundaries (high-wavenumber components). In recent years, Full Waveform Inversion (FWI) has emerged as a robust solution for high-resolution velocity model building. Conventional FWI estimates of the velocity mainly rely on refracted waves that have limited penetration depth controlled by the maximum acquired offset. This has triggered long-offset acquisitions for velocity refinement of deep targets. As an alternative, utilizing reflections with proper scale separation relaxes the depth limitation and enables velocity updates of deep structures (e.g., Xu et al., 2012).

Likewise, Least-Squares Reverse Time Migration (LSRTM) is the method of choice for high-resolution imaging of complex structures. Similar to FWI, data domain LSRTM is an adjoint-state inversion method that aims to minimize the misfit between modeled and recorded data using reflected energy. Accordingly, it is natural to solve both problems in a joint scheme where each inversion targets specific wavenumber components. The scale separation of the gradient is essential for minimizing the crosstalk between the two parameters. A modeling relation with proper parameterization and capability to generate the full acoustic wavefield is equally important.

Previously, approaches to simultaneously invert for velocity and reflectivity have been proposed. Berkhout (2012) introduced a joint migration inversion whereas his approach uses a modeling engine that only considers waves propagating in the up/down directions (Verschuur et al., 2016). Therefore, the estimation of the velocity does not include head and diving waves that can be essential for robust velocity model building. Alternatively, the FWI and LSRTM loops could be employed in a nested fashion (e.g., Cheng et al., 2020), but the cost increase is significant.

We present a novel inversion approach to simultaneously estimate velocity and reflectivity. Our scheme uses a full wavefield modeling relation parameterized in terms of velocity and vector reflectivity (Whitmore et al., 2020). The other fundamental component of our approach is a robust separation of the low- and high-wavenumber contents of the gradient to update velocity and reflectivity, respectively (Whitmore and Crawley, 2012; Ramos-Martinez et al., 2016). With minimally pre-processed input data, the output of the simultaneous inversion is an FWI velocity model together with an accurate estimate of the earth reflectivity that is compensated for incomplete acquisition, poor illumination and multiple crosstalk. We first describe the theory supporting the simultaneous inversion, then we show its performance using two field surveys from the Gulf of Mexico and the Campos Basin in Brazil.

Theory

We use the following wave-equation parametrized in terms of velocity and vector reflectivity as our modeling procedure:

$$\frac{1}{V(\boldsymbol{x})^2}\frac{\partial^2 P(\boldsymbol{x},t)}{\partial t^2} - \nabla^2 P(\boldsymbol{x},t) - \frac{\nabla V(\boldsymbol{x})}{V(\boldsymbol{x})} \cdot \nabla P(\boldsymbol{x},t) + 2\boldsymbol{R}(\boldsymbol{x}) \cdot \nabla P(\boldsymbol{x},t) = S(\boldsymbol{x},t) \qquad (1)$$

where P is the total pressure wavefield which is a function of space ($\boldsymbol{x}$) and time (t), V is the velocity, $\boldsymbol{R}(\boldsymbol{x}) = \frac{1}{2}\frac{\nabla Z(\boldsymbol{x})}{Z(\boldsymbol{x})}$ is the vector reflectivity in which Z is the acoustic impedance and S is the source. Using this representation, velocity and reflectivity are directly set as the model parameters, and there is no need to construct a density model. Equation 1 is essentially equivalent to the variable density wave-equation. Thus, the modeling procedure is able to generate the full acoustic wavefield, including refracted and reflected energy, as well as free-surface and internal multiples (Whitmore et al., 2020).

Velocity and vector reflectivity models are updated using their appropriate kernels after scale separation. The velocity kernel (Ramos-Martinez et al., 2016) is defined as:

$$K_V(\boldsymbol{x}) = \frac{1}{I(\boldsymbol{x})}[\int \left(W_1(\boldsymbol{x},t) \frac{1}{V(\boldsymbol{x},t)^2} \frac{\partial P(\boldsymbol{x},t)}{\partial t} \frac{\partial Q(\boldsymbol{x},t)}{\partial t} - W_2(\boldsymbol{x},t)\nabla P(\boldsymbol{x},t) \cdot \nabla Q(\boldsymbol{x},t) \right) dt], \qquad (2)$$

and the impedance kernel (Whitmore and Crawley, 2012) used for reflectivity update is given as follows:

$$K_Z(\boldsymbol{x}) = \frac{1}{I(\boldsymbol{x})}[\int \left(W_3(\boldsymbol{x},t) \frac{1}{V(\boldsymbol{x},t)^2} \frac{\partial P(\boldsymbol{x},t)}{\partial t} \frac{\partial Q(\boldsymbol{x},t)}{\partial t} + W_4(\boldsymbol{x},t)\nabla P(\boldsymbol{x},t) \cdot \nabla Q(\boldsymbol{x},t) \right) dt], \qquad (3)$$

where $W_i(i = 1,2,3,4)$ are dynamic weights, P and Q are the forward and adjoint wavefields and I is the illumination term. The inversion scheme updates both velocity and reflectivity during each iteration. The simultaneous inversion workflow is summarized in Figure 1. If the reflectivity model is not updated, the flow reduces to an FWI procedure to update the velocity model (Yang et al., 2020). If only the impedance kernel is used, the workflow is then similar to LSRTM.
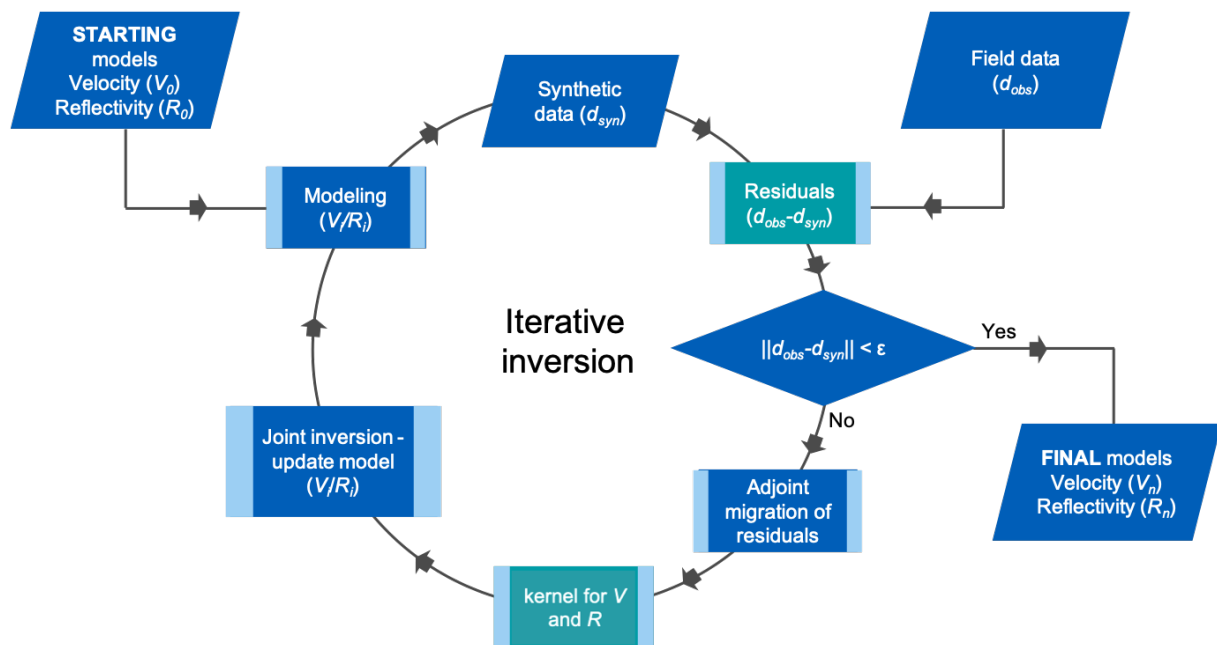

Figure 1 A schematic of the full wavefield velocity and reflectivity simultaneous inversion approach.

Field data examples

We illustrate the benefits of our new simultaneous inversion using two field datasets acquired with multisensor streamers. In both examples, we start from simple initial models and use the total pressure data with minimum pre-processing and a maximum full power frequency of 20 Hz. The kinematics of the initial models are not accurate, but no cycle-skipping is observed at the selected frequency band.

The first field data example is from data acquired in deep-water Gulf of Mexico (Desoto Canyon area). The maximum offset is 12 km. Figure 2a shows the initial velocity model while the initial reflectivity is assumed to be zero. In Figure 2c, we show the reflectivity from the first iteration of the inversion, which is equivalent to performing RTM with the initial model. In this first image, the crosstalk produced by the multiple energy from the unconformity interfering with the deep reflections is indicated by the oval. The results after several iterations of the simultaneous inversion are shown in Figures 2b and 2d. The inverted velocity model overall shows higher resolution. Also, notice coherency enhancements and a clear reduction of the crosstalk in the final reflectivity model.

The second field data example is from a deep-water setting in Campos Basin, offshore Brazil. Although the maximum inline offset acquired in this survey is 10 km, the water column of more than 3 km makes it challenging to update deep targets using refracted energy. We perform our simultaneous inversion scheme using the total pressure data without data selection. In Figures 3a and 3b, we show the vertical reflectivity models corresponding to the first and final iteration of the inversion, respectively. Velocity updates are displayed in Figure 3c on top of the final vertical reflectivity. The maximum depth of velocity update is beyond the maximum penetration depth provided by the diving waves. Note the improvement in the resolution of the shallow fault system after inversion. Moreover, there are coherency enhancements in the deep reflectors of the mini-basin and the steep salt flanks. In Figure 3d, we show the final horizontal reflectivity image which mainly concentrates around those steep salt flanks. QC of results is supported by the image gathers computed for the initial and the final velocity model from the simultaneous inversion, which are shown in Figures 3e and 3f, respectively.
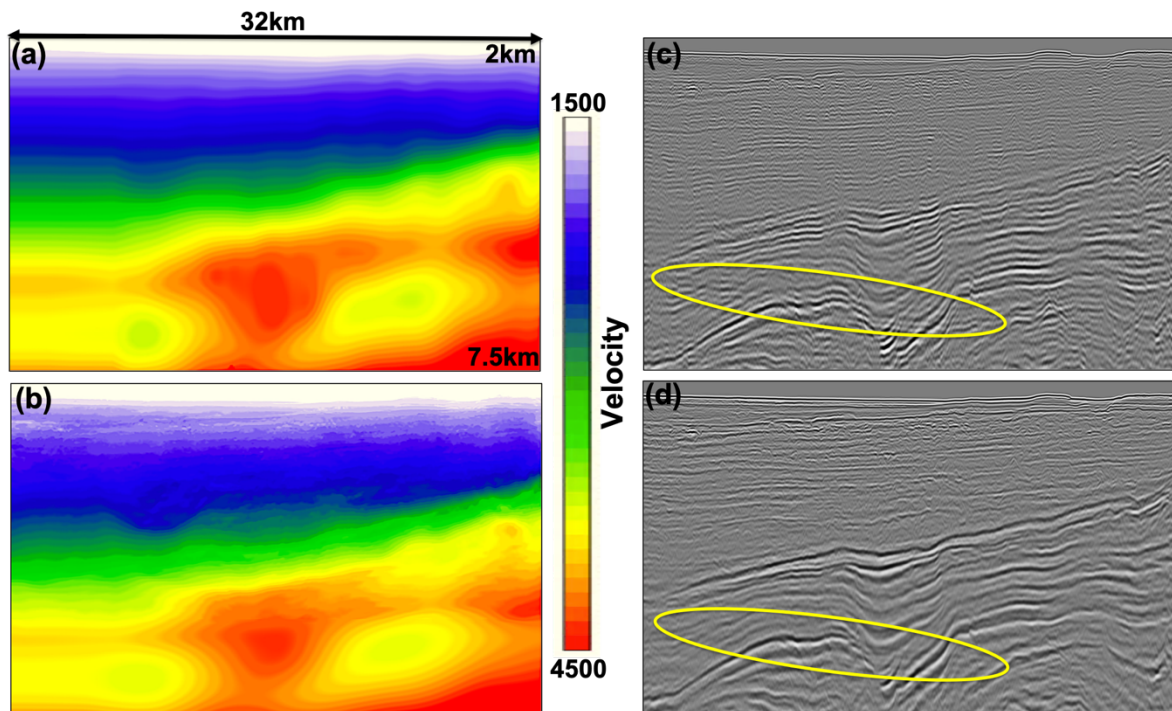

Figure 2 *Desoto Canyon field data example. (a) Initial and (b) inverted velocity models. (c) First iteration and (d) final vertical reflectivity. Notice the crosstalk reduction as the yellow oval indicates.*

Conclusions

We introduced a non-linear iterative inversion solution to simultaneously estimate velocity and reflectivity. The method is based on two developments that facilitate robust multi-parameter inversion: 1) a wave-equation modeling relation parameterized in velocity and vector reflectivity and 2) a robust procedure to separate the low- and high-wavenumber components of the inversion gradient. We successfully applied our workflow to two field datasets. Results demonstrated that while the velocity model is iteratively updated, an accurate estimate of the earth reflectivity is simultaneously generated. We demonstrated that FWI and LSRTM can be performed jointly as a single inversion workflow, with significant reduction in turnaround time for the model building and imaging project.

Acknowledgments

References

Berkhout, A. J. [2012] Combining full wavefield migration and full waveform inversion, a glance into the future of seismic imaging. *Geophysics*, **77**(2), 43-50.

Cheng, J., Wang, T., and Xu, W. [2020] Hessian Based Reflection Waveform Inversion. *82nd EAGE Conference & Exhibition,* Extended Abstracts, 1-5.

Ramos-Martinez, J., Crawley, S., Zou, K., Valenciano, A.A., Qiu, L. and Chemingui, N. [2016] A robust gradient for long wavelength FWI updates. *78th EAGE Conference & Exhibition,* Extended Abstracts, 1-5.

Verschuur, D.J., Staal, X.R. and Berkhout, A. J. [2016] Joint migration inversion: Simultaneous determination of velocity fields and depth images using all orders of scattering. *The Leading Edge*, **35**(12), 1037-1046.

Whitmore, N.D., Ramos-Martinez, J., Yang Y. and Valenciano, A.A. [2020] Full wave field modeling with vector-reflectivity. *82nd EAGE Conference & Exhibition,* Extended Abstracts, 1-5.

Whitmore, N. D. and Crawley S. [2012] Application of RTM inverse scattering imaging conditions. *82nd Annual International Meeting, SEG,* Expanded Abstracts, 1-6.

Xu, S., Wang, D., Chen, F., Zhang, Y. and Lambaré, G. [2012] Full waveform inversion for reflected seismic data. *74th EAGE Conference & Exhibition,* Extended Abstracts, W024.

Yang, Y., Ramos-Martinez, J., Whitmore, D., Valenciano, A.A. and Chemingui N. [2020] Full Waveform Inversion Using Wave Equation Reflectivity Modeling. *82nd EAGE Conference & Exhibition,* Extended Abstracts, 1-5.
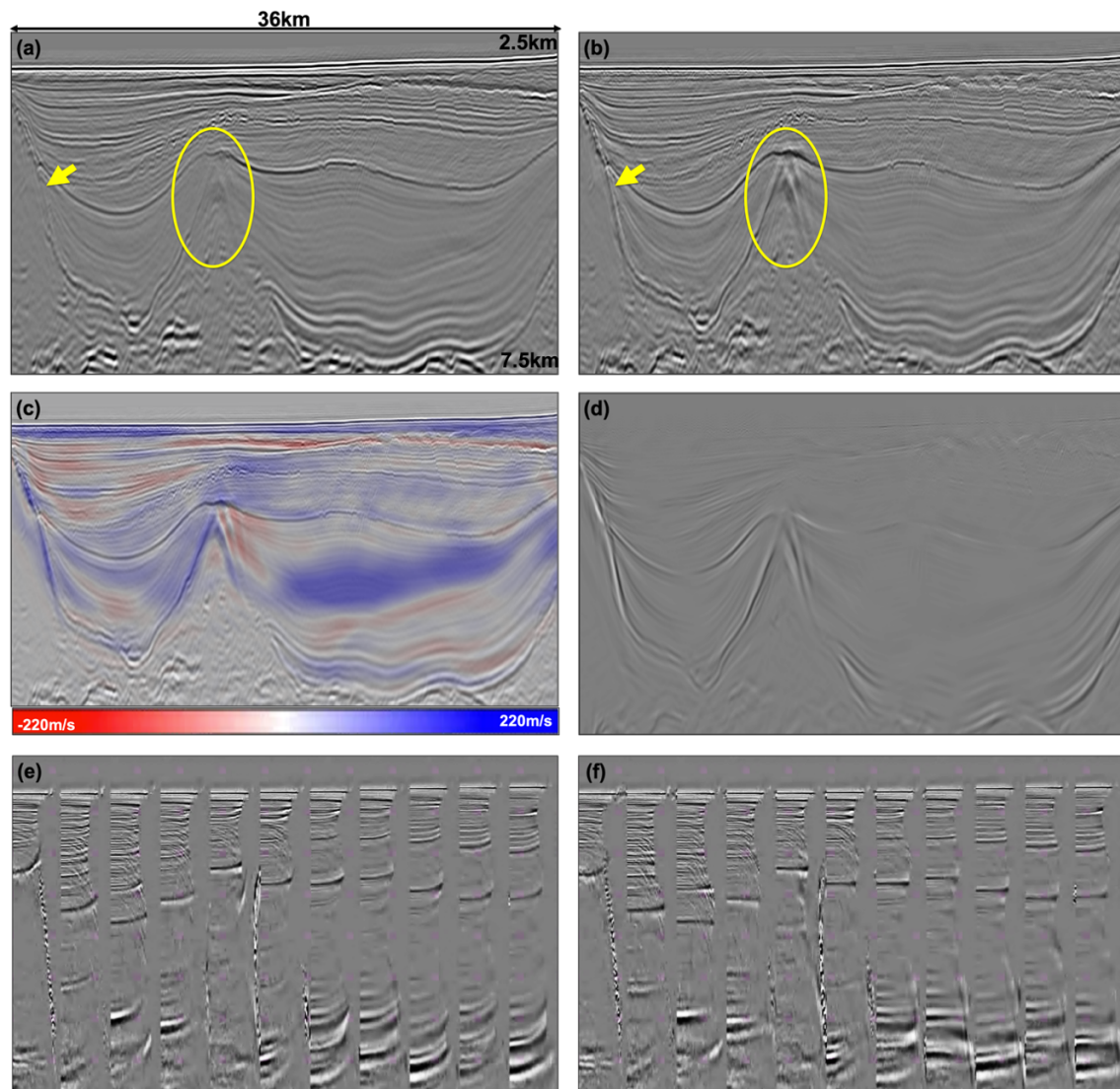
Figure 3 *Campos Basin field data example. (a) Vertical reflectivity from the first iteration. (b) Final inverted vertical reflectivity. (c) Velocity updates on final vertical reflectivity. (d) Final horizontal reflectivity along inline direction. Image gathers from the initial model (e) and the FWI model (f).*